

AFRL-ML-WP-TR-1999-4009

**EXPLORATORY NONDESTRUCTIVE
EVALUATION (NDE) RESEARCH FOR
ADVANCED MATERIALS AND PROCESSES**

**VOLUME 1 : HIGH RESOLUTION COMPUTED
TOMOGRAPHY FOR FAILURE ANALYSIS**



**RICHARD BOSSI
BENJAMIN KNUTSON
ROBERT NERENBERG**

**LYLE DEOBALD
JAMES NELSON
WILLIAM SHEPHERD**

**BOEING INFORMATION
SPACE & DEFENSE SYSTEMS
P.O.BOX 3999
SEATTLE, WA 98124**

JULY 1998

FINAL REPORT FOR 07/01/1995 – 04/30/1998

APPROVED FOR PUBLIC RELEASE; DISTRIBUTION UNLIMITED

**MATERIALS AND MANUFACTURING DIRECTORATE
AIR FORCE RESEARCH LABORATORY
AIR FORCE MATERIEL COMMAND
WRIGHT-PATTERSON AIR FORCE BASE OH 45433-7734**

19990726 051

DTIC QUALITY INSPECTED 4

NOTICE

WHEN GOVERNMENT DRAWINGS, SPECIFICATIONS, OR OTHER DATA ARE USED FOR ANY PURPOSE OTHER THAN IN CONNECTION WITH A DEFINITELY GOVERNMENT-RELATED PROCUREMENT, THE UNITED STATES GOVERNMENT INCURS NO RESPONSIBILITY OR ANY OBLIGATION WHATSOEVER. THE FACT THAT THE GOVERNMENT MAY HAVE FORMULATED OR IN ANY WAY SUPPLIED THE SAID DRAWINGS, SPECIFICATIONS, OR OTHER DATA, IS NOT TO BE REGARDED BY IMPLICATION OR OTHERWISE IN ANY MANNER CONSTRUED, AS LICENSING THE HOLDER OR ANY OTHER PERSON OR CORPORATION, OR AS CONVEYING ANY RIGHTS OR PERMISSION TO MANUFACTURE, USE, OR SELL ANY PATENTED INVENTION THAT MAY IN ANY WAY BE RELATED THERETO.

THIS REPORT IS RELEASABLE TO THE NATIONAL TECHNICAL INFORMATION SERVICE (NTIS). AT NTIS, IT WILL BE AVAILABLE TO THE GENERAL PUBLIC, INCLUDING FOREIGN NATIONS.

THIS TECHNICAL REPORT HAS BEEN REVIEWED AND IS APPROVED FOR PUBLICATION.



CHARLES F. BUYNAC, Project Engineer
Nondestructive Evaluations Branch
Metals, Ceramics & NDE Division



THOMAS J. MORAN, Acting Chief
Nondestructive Evaluations Branch
Metals, Ceramics & NDE Division



GERALD J. PETRAK, Assistant Chief
Metals, Ceramics & NDE Division
Materials & Manufacturing Directorate

IF YOUR ADDRESS HAS CHANGED, IF YOU WISH TO BE REMOVED FROM OUR MAILING LIST, OR IF THE ADDRESSEE IS NO LONGER EMPLOYED BY YOUR ORGANIZATION, PLEASE NOTIFY, AFRL/MLLP, WRIGHT-PATTERSON AFB OH 45433-7817 AT (937) 255-9819 TO HELP US MAINTAIN A CURRENT MAILING LIST.

COPIES OF THIS REPORT SHOULD NOT BE RETURNED UNLESS RETURN IS REQUIRED BY SECURITY CONSIDERATIONS, CONTRACTUAL OBLIGATIONS, OR NOTICE ON A SPECIFIC DOCUMENT.

REPORT DOCUMENTATION PAGEFORM APPROVED
OMB NO. 0704-0188

Public reporting burden for this collection of information is estimated to average 1 hour per response, including the time for reviewing instructions, searching existing data sources, gathering and maintaining the data needed, and completing and reviewing the collection of information. Send comments regarding this burden estimate or any other aspect of this collection of information, including suggestions for reducing this burden, to Washington Headquarters Services, Directorate for Information Operations and Reports, 1215 Jefferson Davis Highway, Suite 1204, Arlington, VA 22202-4302 and to the Office of Management and Budget, Paperwork Reduction Project (0704-0188), Washington, DC 20503.

| | | | | |
|---|--|--|---|--|
| 1. AGENCY USE ONLY (Leave blank) | | 2. REPORT DATE JULY 1998 | 3. REPORT TYPE AND DATES COVERED FINAL REPORT FOR 07/01/1995-04/30/1998 | |
| 4. TITLE AND SUBTITLE EXPLORATORY NONDESTRUCTIVE EVALUATION (NDE) RESEARCH FOR ADVANCED MATERIALS AND PROCESSES; VOLUME 1: HIGH RESOLUTION COMPUTED TOMOGRAPHY FOR FAILURE ANALYSIS | | | 5. FUNDING NUMBERS C - F33615-95-C-5225 PE - 62102F PR - 4349 TA - 44 WU - 01 | |
| 6. AUTHOR(S) RICHARD BOSSI, LYLE DEOBALD, BENJAMIN KNUTSON, JAMES NELSON, ROBERT NERENBERG, AND WILLIAM SHEPHERD | | | 8. PERFORMING ORGANIZATION REPORT NUMBER D950-10333-1 | |
| 7. PERFORMING ORGANIZATION NAMES(S) AND ADDRESS(ES) BOEING INFORMATION SPACE & DEFENSE SYSTEMS P.O. BOX 3999 SEATTLE, WA 98124 | | | | |
| 9. SPONSORING/MONITORING AGENCY NAMES(ES) AND ADDRESS(ES) MATERIALS & MANUFACTURING DIRECTORATE AIR FORCE RESEARCH LABORATORY AIR FORCE MATERIAL COMMAND WRIGHT-PATTERSON AFB OH 45433-7734 | | | 10. SPONSORING/MONITOR- ING AGENCY REPORT NUMBER AFRL-ML-WP-TR-1999-4009 | |
| 11. SUPPLEMENTARY NOTES POC: CHARLES F. BUYNAC, AFRL/MLLP, 59807 | | | | |
| 12a. DISTRIBUTION/AVAILABILITY STATEMENT APPROVED FOR PUBLIC RELEASE: DISTRIBUTION IS UNLIMITED | | | 12b. DISTRIBUTION CODE | |
| 13. ABSTRACT (Maximum 200 words) High Resolution Computed Tomography (CT) for Failure Analysis: Failure analysis is an essential element of all engineered products. The goal of failure analysis is the understanding of root causes of any undesirable effects. High resolution computed tomography offers detailed information on the internal assembly and material condition of objects under failure analysis investigation allowing accurate interpretation of effects not detectable by other means. Failure analysis using CT investigations are improved in technical accuracy at a reduced schedule and cost over alternative approaches. The cost of a high resolution CT system is often difficult to justify for CT applications only. However, when the system provides high resolution radioscopic imaging as well as CT, the cost justification is favorable. To achieve a combination high resolution radioscopic and CT system, a microfocus X-ray source is used. A versatile microfocus radioscopic system with CT capability has been successfully implemented as a standard tool in an aerospace failure analysis laboratory whose budget is in the range of \$1 M/year. Using this tool, studies of electronic, electromechanical and composite material items have been performed. Such a system pays for itself within 2 years through higher productivity of the laboratory, increased laboratory value to the company and timely resolution of critical problems. | | | | |
| 14. SUBJECT TERMS Failure Analysis, X-ray, Imaging, Microfocus, Radioscopy, Computed Tomography, Electronics, Composites, Area Inspection, Shearography, Interactive Multimedia Based Training, Computer-Managed Instruction, Nondestructive Evaluation and Inspection | | | 15. NUMBER OF PAGES 154 | |
| 17. SECURITY CLASSIFICATION OF REPORT Unclassified | | | 16. PRICE CODE | |
| | | | 20. LIMITATION OF ABSTRACT SAR | |
| 18. SECURITY CLASSIFICATION OF THIS PAGE Unclassified | | 19. SECURITY CLASSIFICATION OF ABSTRACT Unclassified | | |

NSN 7540-01-280-5500

COMPUTER GENERATED

STANDARD FORM 298 (Rev. 2-89)
Prescribed by ANSI Std. Z39-18
298-102

TABLE OF CONTENTS

| <u>Section</u> | <u>Page</u> |
|---|-------------|
| LIST OF FIGURES | IV |
| ACKNOWLEDGEMENTS | V |
| DISCLAIMER | V |
| EXECUTIVE SUMMARY | 1 |
| 1.0 INTRODUCTION | 3 |
| 2.0 MICROFOCUS RADIOSCOPY/COMPUTED TOMOGRAPHY SYSTEM | 4 |
| 3.0 FAILURE ANALYSIS EXAMPLES | 9 |
| 3.1 Switches, Relays, Electrical Components & Systems | 9 |
| 3.2 Connectors And Fiber Optics | 14 |
| 3.3 Composite And Metallic Structure | 16 |
| 4.0 COST BENEFIT ANALYSIS | 19 |
| 5.0 RECOMMENDATIONS | 22 |
| 6.0 REFERENCES | 23 |

LIST OF FIGURES

| <u>Figure</u> | <u>Page</u> |
|---|-------------|
| Figure 2.1. Microfocus radioscopy and CT system | 4 |
| Figure 2.2. MCT Nominal System Imaging Characteristics | 5 |
| Figure 2-3. Radioscopic image of an integrated circuit showing 0.025 mm diameter gold wires bonded to the chip | 6 |
| Figure 2-4. Comparison of radiography and computed tomography | 7 |
| Figure 2-5. Comparison of effective beam width designs for CT | 8 |
| Figure 2-6. High resolution CT image of line pair gauge | 8 |
| Figure 3.1. Edge enhanced radioscopic image of relay | 9 |
| Figure 3.2. Solid state relay with a missing wire | 10 |
| Figure 3.3. Radioscopic image of a wire wound resistor (approximately 1 mm diameter coil) showing improper spacing | 11 |
| Figure 3.4. Photograph of an aircraft temperature sensor | 12 |
| Figure 3.5. Radioscopic image of a temperature sensor showing a broken wire | 12 |
| Figure 3.6. Radioscopic image of a temperature sensor showing a wire near a lead | 13 |
| Figure 3.7. CT contiguous image sequence showing the temperature sensor wire fail to connect to the lead | 13 |
| Figure 3.8. Configuration of high resolution CT to evaluate a fiber optic connection | 14 |
| Figure 3.9. CT data from a fiber optic splice | 15 |
| Figure 3.10. CT data from a fiber optic splice showing MPR views of two bad splices | 15 |
| Figure 3.11. CT data from a composite sample | 16 |
| Figure 3.12. CT scan of rivet a) pre sectioning and b) post sectioning | 17 |
| Figure 3.13. CT slice through the reservoir showing the crack | 18 |
| Figure 3.14. MPR of the crack in the reservoir | 18 |
| Figure 4.1. Simple cost benefit payback techniques for MRCT system | 20 |

ACKNOWLEDGEMENTS

High Resolution CT for Failure Analysis. Technical effort in this program was supported by Reid Mickelsen and Dan Cross of the Boeing Failure Analysis Laboratory, Bob Carlsen and Jim Nelson of the Boeing Physics staff and Gary Georgeson of Boeing MR&D.

DISCLAIMER

The information contained in this document is neither an endorsement nor criticism of any software applications, computer hardware, imaging instrumentation or other equipment used in this study.

EXECUTIVE SUMMARY

Boeing Defense & Space Group was awarded the "Exploratory Nondestructive Evaluation (NDE) Research for Advanced Materials and Processes" contract in 1995 to study improvements for NDE methods for evaluating aging assets, primarily aircraft, with the primary end objective to reduce the cost of maintaining these aging assets.

The study involved three separate approaches, responsive to the three task elements contained in the Statement of Work. The first approach was to look at the use of high resolution computed tomography (CT) in failure analysis, the second was to study improvements in shearography, and the third was a demonstration of the use of interactive multimedia computer-based training for NDE/I inspectors. Because each task is distinctly unique, they are discussed in separate report volumes – collectively referred to as FAST: Failure Analysis, Shearography, Training. This is volume I, covering Failure Analysis.

Under the "Exploratory Nondestructive Evaluation (NDE) Research for Advanced Materials and Processes" contract, the applicability of high resolution computed tomography (CT) has been evaluated for its benefits to aerospace equipment and materials failure analysis. Failure analysis is an essential element of all engineered products. The goal of failure analysis is the understanding of the root causes of any undesirable effects. High resolution computed tomography offers detailed information on the internal assembly and material condition of objects under failure analysis investigation allowing accurate interpretation of effects not detectable by other means. Failure analysis investigations are improved in technical accuracy at a reduced schedule and cost over alternative approaches. The cost of a high resolution CT system is, however, very difficult to justify on its own. Such systems typically would cost over \$0.5M. To obtain adequate return on investment the CT applications requirements would need to be considerable, (i.e., 50 to 100 jobs per year).

However, combining CT with a high resolution microfocus based radioscopy system provides more than adequate justification for implementation. The microfocus X-ray source is the key to the success of this system for both radioscopy and CT. Failure analysis has a reasonably high requirement for X-ray inspection, which increases in applicability if very high resolution can be obtained. With a microfocus source, projection magnification can be employed for imaging without the detriment of geometric unsharpness found in conventional X-ray source spot imaging. The magnification enlarges the detail in the object so that an image intensifier detector system can be used, allowing images to be viewed in real-time or near real-time on a video display. With the projection magnification the inherent resolution of the image intensifier (which is much poorer than X-ray film) is more than sufficient to resolve fine detail of interest in a test object. In fact, with a very high quality spot size, magnifications of 20 to 50 X can be used to image very fine detail that would not be imaged with X-ray film. The detriment to using high magnification is the limitation in the field of view of the object. For most failure analysis investigations this is not a problem.

The improved productivity of microfocus radioscopy over film studies in a failure analysis laboratory justifies the acquisition of the source and detector system. The addition of CT to the system is a small cost (usually less than 20%) of the total system value and provides a

tool to solve unique problems that may occur sporadically (10 to 20 times per year). A versatile microfocus radioscopic system with CT capability can pay for itself within 2 years through higher productivity of the laboratory, increased laboratory value to the company and resolution of critical component problems whose worth exceeds the cost of the microfocus radioscscopy/CT (MRCT) system. Because MRCT offers detailed information on internal object assembly and material condition, the overall failure analysis investigation effort is reduced while improving the failure analysis assessment accuracy. Such MRCT systems become the first step in a failure analysis study to assess the condition prior to any mechanical damage that may be performed on the part. It is not uncommon to be able to complete an analysis based on these data alone. The speed of assessment is often critical in some studies. The schedule savings for critical programs, by MRCT capability for failure analysis, has been estimated to save several millions of dollars per year.

Under this program the information obtained in the evaluation of applications for MRCT in failure analysis has been distributed to government and industry. Three presentations with published technical paper proceedings have been made on the topic to JANNAF, SPIE and ISTFA, and a presentation was made at the ASNT 1998 Fall Conference. A paper is in review for publication in the *Journal of Testing and Evaluation*.

1.0 INTRODUCTION

In large aerospace companies, failure analysis is performed by dedicated organizations equipped with tools for electronic testing, mechanical testing, sectioning, photography, micrographic examination, electron microscopy and X-ray examination capability. Failure analysis evaluation is an essential process which leads to improvements in the materials, designs and manufacturing technology that go into advanced aerospace systems. Having the appropriate tools to perform the investigations is a critical characteristic of failure analysis laboratories.

In the past, X-ray examination has been performed using small cabinet X-ray systems with dry film. These systems are used to record the interior configuration of components looking for connections, contacts, gaps, etc. Each view of the object requires a setup and an exposure. The films are often used in reports to document the internal part condition, as part of the failure analysis investigation. The data may also be used as a guide to further destructive analysis tests. These types of X-ray systems are relatively inexpensive, less than \$30,000. The cost of operation is low and the cost of film supply is not very expensive, perhaps on the order of \$1 per sheet. Using dry print film systems, such as Polaroid, avoids the costs of chemicals and darkroom facilities required for conventional X-ray film radiography. The detailed sensitivity of the dry print film systems is not as high as can be obtained with standard X-ray film. However, besides the difficulties of darkroom processing, X-ray film is very hard to include in reports without printing or digitization apparatus. Failure analysis laboratories have engaged in film radiography and maintain darkroom facilities and chemicals, but they are used reluctantly.

Improvements over conventional X-ray film evaluation of components for failure analysis are available. Computed tomography, can be used to obtain cross sectional images of components revealing features that are not detectable by other means. Radioscopic imaging can be performed to observe items as they function, or to use image processing schemes such as subtraction and edge enhancement to detect internal details and configurations. The drawback to the use of these technologies has been the general requirement for high resolution to detect small features (i.e., 0.025 to 0.25 mm) in size in objects that are relatively small (i.e., 5 to 50 mm) in size. An X-ray imaging technique which provides very high resolution images is microfocus radioscopy (1). The radioscopy capability allows the object under examination to be manipulated while being observed on a television monitor (2). The projection magnification capability of a high quality microfocus X-ray source allows very high resolution imaging. The fundamental capability of a radioscopy manipulator stage and imaging system allows the ready implementation of data acquisition and reconstruction for computed tomography (CT) imaging. The CT cross sectional image shows the object interior without the confusion of superposition of projected features in the radiographic or radioscopy view (3-5). A series of CT slices through the object can be combined to show the three-dimensional spatial distribution of material in the component under test for assessment of internal configuration and material condition nondestructively. Radioscopy and CT can be used to make internal dimensional measurements of features easier than radiography and with equivalent or superior resolution.

2.0 MICROFOCUS RADIOGRAPHY/COMPUTED TOMOGRAPHY SYSTEM

An example of a combined microfocus radioscopic and CT (MRCT) system is a unit acquired for the Boeing Phantom Works, Failure Analysis Laboratory (6). The system is a BIR ACTIS 300 with a Fein Focus 160 kV source. Figure 2.1 shows the configuration. The system footprint and work area in a laboratory requires approximately 3.6 x 3.6m (12 feet x 12 feet) of floor space. The source is installed, fixed in space, in a cabinet. The spot size is nominally less than 10 micrometers. The object is placed on a precision part manipulator stage (0.01 mm linear motion measurement, 0.01 degree rotation measurement) that can handle objects of up to 10 kg weight and 500 x 500 x 500 mm in size. The stage has five axes of motion: turntable rotation, linear motions in X, Y, Z and tilt angle. The image intensifier, aligned with the X-ray spot in X and Y has motion capability toward and away from the source in Z. The intensifier has three image field sizes, 220 mm (9"), 175 mm (7") and 110 mm (4.5"). The manufacturer rated resolution of the intensifier is 5.0, 5.6 and 6.8 line pair/mm respectively for each field of view. A 760 by 520 CCD camera is focused on the output of the image intensifier using a remote control zoom lens. The CCD camera output goes to an image processor and video display. The output is also sent to the input to a CT data acquisition system. In this case a line of data across the CCD array is used as the input for each projection of a CT slice. Multiple lines may be used depending on the effective slice width of the CT image desired. Third generation CT scan data acquisition is employed by rotating the turntable (5).

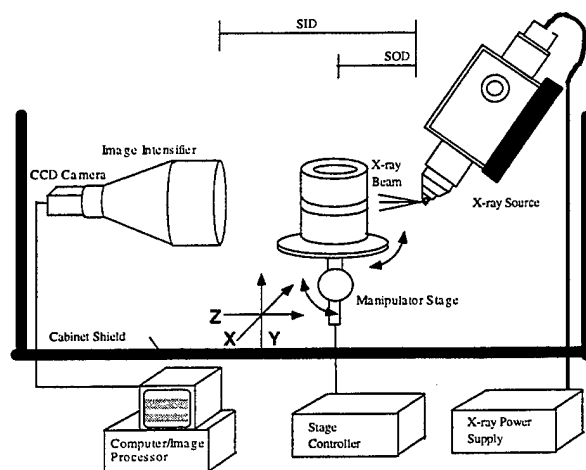


Figure 2.1. Microfocus radiography and CT system

The nominal imaging characteristics of the described MRCT system are listed in Figure 2.2. These values are dependent on the object size, field of view and imaging times. For radiography, obtaining images of details in the range of 0.025 mm, or 20 line pairs per millimeter (lp/mm) is relatively easy to accomplish because of the ability to use high magnifications with small geometric unsharpness. Sensitivity to better than 1% is possible using image averaging data acquisition techniques, field flattening, low kV and high current. For CT the resolution is dependent on the field of view used. The reconstructed image size is

512 x 512 so details of one to two parts in 500 are imaged. For greater than 8 line pair/mm resolution, the objects must be small, less than 10 mm in diameter.

| | |
|---------------------|-----------------------|
| Radioscopy | |
| Resolution: | >20 lp/mm (<0.025 mm) |
| Sensitivity: | < 1% |
| Computed Tomography | |
| Resolution: | > 8 lp/mm (<0.060 mm) |
| Sensitivity | <1% |
| Slice Thickness: | down to 0.050 mm |
| Slice Steps: | down to 0.050 mm |
| Scan Speed: | 1 slice/minute |

Figure 2.2. MCT Nominal System Imaging Characteristics

The microfocus source is the key to the success of MRCT systems used in failure analysis investigation for both radioscopy and CT. With the microfocus source, projection magnification can be employed for imaging without the detriment of geometric unsharpness which would occur with a conventional X-ray source due to the spot size. The magnification enlarges the detail in the object so that the image intensifier detector's inherent resolution (which is much poorer than X-ray film) is sufficient to resolve the detail of interest. In fact, with a very high quality spot size, magnifications of 20 to 50 X can be used to image very fine detail that would not be imaged with film. The magnification is given by:

$$M = \text{SID}/\text{SOD}$$

where SID is the source to image distance and SOD is the source to object distance. The unsharpness in an image will be a combination of the unsharpness of the detector and the unsharpness due to the geometry (7). The unsharpness due to the geometry is given by:

$$U_g = s(\text{SID} - \text{SOD})/\text{SOD}$$

or

$$U_g = s(M-1)$$

where s is the spot size of the X-ray source. As the difference between the SOD and SID increases, M increases and U_g increases. But if s is very small, then U_g will not necessarily increase significantly relative to the inherent unsharpness of the detector screen (U_d). For example, a typical U_d for a radioscopy system may be in the range of 0.05 to 0.2 mm. For the U_g value to reach 0.2 mm unsharpness with a 0.005 mm focal spot size, the magnification would have to be 39. At a magnification of 39, features on the order of 0.025 mm (0.001 inch) are approximately 1 mm in size and can be readily resolved with radioscopy imaging systems that have U_d values in the range of 0.05 to 0.2 mm previously noted. Figure 2.3 demonstrates this by showing the 0.025 mm gold wire bonds in an integrated circuit (IC) package using very high magnification. This image is actually used as a means of tuning the microfocus source by optimizing the sharpness of the wires.

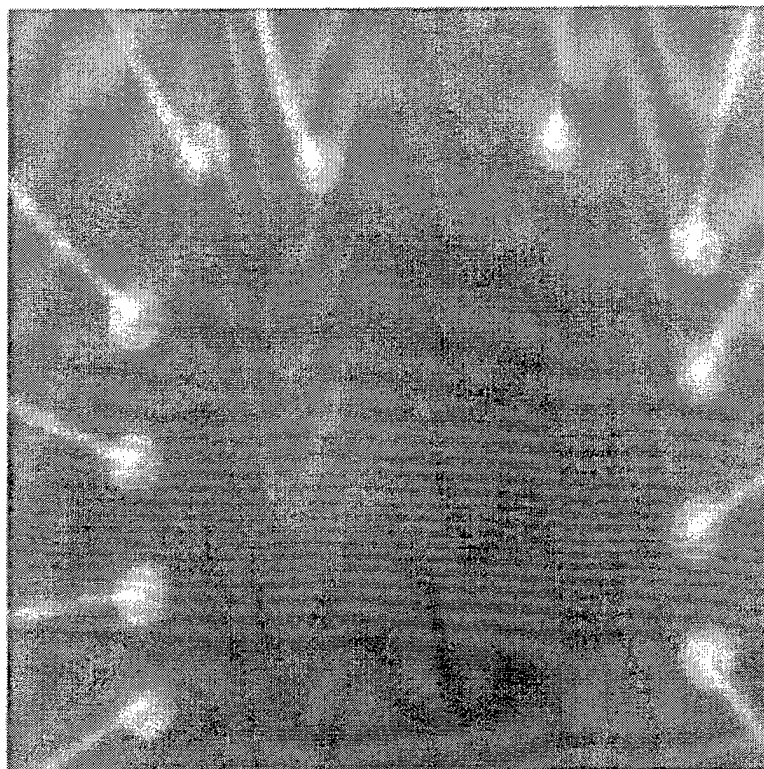
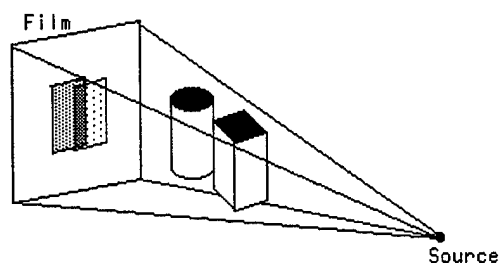


Figure 2-3. Radioscopic image of an integrated circuit showing 0.025 mm diameter gold wires bonded to the chip

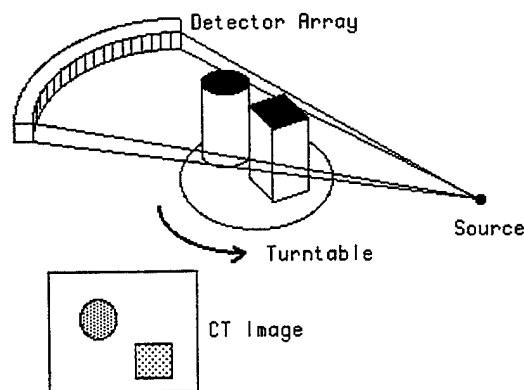
The projection magnification process moves the object away from the intensifier so that in addition to the increase in the size of the object at the detector, the radiation scatter noise from the object is not as readily detected. This is an advantage over conventional X-ray setups where the object is adjacent to the detection film. The projection magnification configuration results in improved contrast sensitivity. The loss of X-ray intensity which occurs due to the microfocus spot, relative to conventional x-ray tubes, is compensated by the gain of the intensifier and the use of smaller SID's. Statistical noise can be reduced by frame averaging in the image processor. Overall, using a radioscopic system in an optimized configuration can result in detail sensitivity superior to the best X-ray film technique (8). The digital picture from the radioscopy image can be directly imported into a report. The live video image can be recorded on videotape, while the object is manipulated in the X-ray beam. One significant drawback to the image intensifier is a variation in intensity across the field of view and there can be a noise pattern on the intensifier screen with age. Image intensifiers have a curved input surface (convex with respect to the source position) that results in an inherent intensity variation across the image. This effect becomes more pronounced with small SID's. Field flattening corrections can be used to reduce this effect.

The CT process offers a further enhancement to imaging capability of a radioscopic system (9-11). Figure 2.4 shows the difference between the radiographic imaging and CT imaging. The radiographic process creates a two-dimensional shadowgraph of the three-dimensional object compressing the total object information into the image. CT uses the measurement of transmitted radiation intensity from many angles about an object to reconstruct image cross

sections of that object. The image is a 2-dimensional plane taken from the 3-dimensional object. By taking a series of CT slices, the entire object can be evaluated. The clear images of interior planes of an object are achieved without the confusion of superposition of features often found with conventional film radiography. The CT images are maps of the relative linear X-ray attenuation coefficient of small volume elements in the object. The X-ray linear attenuation coefficient measurement is directly related to material density and is a function of the atomic number in the small volume elements (voxels). The voxels are defined by the reconstruction matrix (in combination with the X-ray beam width) and by the effective CT slice height. The CT results can provide quantitative information about the density/constituents and dimensions of the features imaged.



Conventional radiography creates a shadowgraph image on film.



Computed tomography reconstructs a cross section image of the interior of the object.

Figure 2-4. Comparison of radiography and computed tomography

The key characteristics of a CT system are the X-ray source energy and size, the detector size, the spacing between the source object and detector, the object material and size, the number of projections taken through the object and the reconstruction matrix size. The resolution of CT systems is determined by the effective x-ray beam width in the object. Figure 2.5 demonstrates the effective beam width in a conventional CT system and a high resolution system using a microfocus source (12).

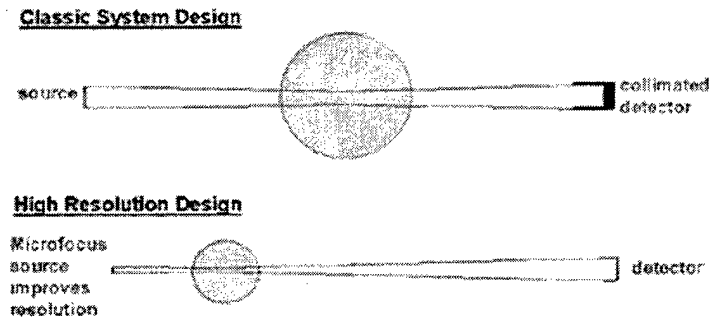


Figure 2-5. Comparison of effective beam width designs for CT

In the first case, the object is normally positioned midway between the source and detector. The effective X-ray beam necks down to minimum at the center if the source size and detector size are about the same. Inherent resolution in this case is only gained by having a small source and small detector. An effective alternative is to use a microfocus source and place the object as close as possible to the source, as shown in the high resolution design of figure 2.5. The effect is to reduce the effective beam size in the part. This technique allows the use of relatively poor resolution detector systems (which can be inexpensive) because of the magnification effect. The limitation in this method is the part size that can be handled. As the part is brought closer to the source the projected size can be allowed to increase only until the detector field of view is filled. Small parts can be highly magnified but larger parts cannot. For a typical maximum detector size of approximately 220 mm, a 50 X magnification could be obtained on a 4 mm size object, while a 40 mm size object would only be allowed a 5X magnification.

An example of this magnification effect is the image of a resolution gauge taken with the microfocus source, shown in Figure 2.6. The resolution gauge contains line pairs from 2 lp/mm down to 16 lp/mm. The system clearly resolves 8 lp/mm and has some sensitivity at 16 lp/mm. In this image the projection magnification is such that the maximum field of view is only 10 mm and the reconstruction matrix is only 2.6 mm. Such imaging parameters are often acceptable on very small components in electronic systems.

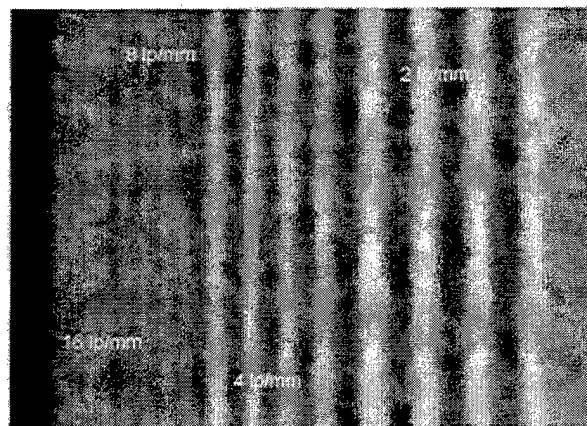


Figure 2-6. High resolution CT image of line pair gauge

3.0 FAILURE ANALYSIS EXAMPLES

The largest area for use of MRCT in failure analysis studies has been in the evaluation of electronic/electromechanical components. Failure analysis studies of these items usually require high resolution imaging systems for relatively small (less than 50-mm-diameter) components. Material studies have also benefited significantly from the high resolution capability of the MRCT system. A few examples are discussed here. Reproduction has reduced the image detail from the original data.

3.1 Switches, Relays, Electrical Components & Systems

Problems with electrical relays are a common category of failure analysis investigations which take advantage of radiosopic imaging to show the condition of the relay in real-time. The relay can be mounted in the X-ray chamber and observed while it functions. This has proved extremely valuable for diagnosing problems in relays, particularly intermittent problems. Prior to the availability of the radiosopic system, the relay cans would be opened and then functioned. This, however, presented a number of concerns about the changes in the operating environment resulting from opening the cans. With radioscopy the relays' internal performance is observed completely nondestructively. Studies on relays using the microfocus radioscopy system have saved numerous hours of alternative testing and resulted in rapid analysis of problems. A common result is to find internal items, which block the functioning of the relay. If the relay is opened, there is a high risk that the blocking material will move or be lost prior to solving the problem. Figure 3.1 shows an example of a radiosopic image of a relay. The approximately 0.1 mm thick contacts are readily detected. One particularly useful technique to detect whether or not the contacts touch is to cycle the switch and to store images of the contacts open and closed. By subtracting the two images the slightest change in the stationary contact will be detected which indicates that a mechanical contact has been made.

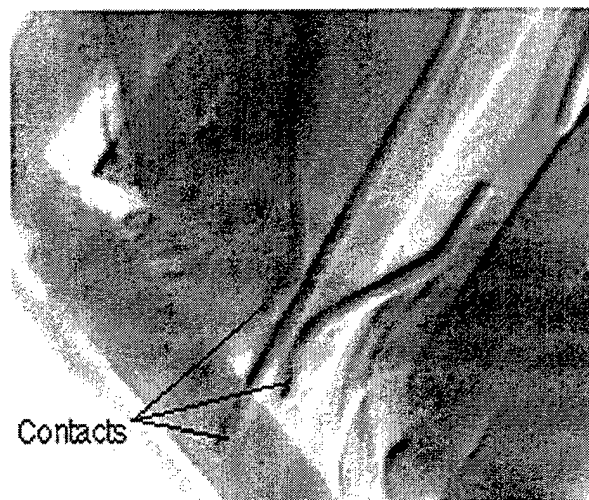


Figure 3.1. Edge enhanced radiosopic image of relay

Another example shows the use of very high magnification to identify a missing wire in a solid state relay. Figure 3.2 shows the radioscopic image with the missing wire bond identified.

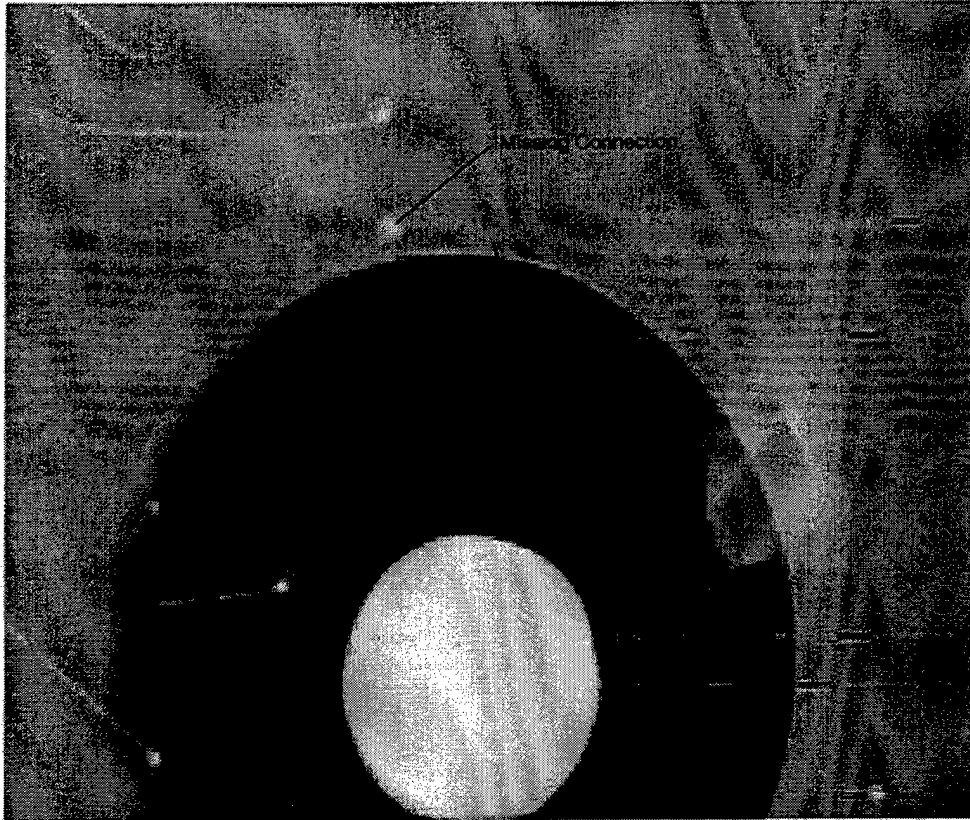


Figure 3.2. Solid state relay with a missing wire

Switches are often similar in physical characteristics to relays, so radioscopy is similarly performed. However, the functioning of switches cannot be performed under X-ray examination unless a robot is used. A robotic manipulator, which has the capability to function the switch while it is being examined in the radioscopic systems, would be a very useful tool in a failure analysis facility.

In addition to radioscopy on relays and switches, CT has been used to measure internal details. In one particular case, the failure analysis investigation of a switch malfunction was performed as part of a multimillion dollar litigation. The ability of CT to resolve the cause of the switch failure (the mechanism would hangup on an internal surface) and absolve the company, compensated for the acquisition of the MRCT system many times over.

Electrical components such as capacitors, resistors, inductors, hybrid chips, transistors, fuses, diodes, light bulbs, SCR's, thermistors, isolators, etc., have all been investigated using MRCT. Figure 3.3 shows a radioscopic image of a wire wound resistor used to detect improper spacing of the wire loops on the approximately 1-mm diameter coil. The

radioscopic image is used to check that no shorting is occurring in the wire windings of the resistor. The MRCT has proved very valuable in the evaluation of such components. In cases of wire wound resistors and inductors, radioscopy has been used for screening purposes on critical missions or program activities where the value of assuring that the components are correct far exceeds the cost of the examination and, in fact, the cost of the entire MRCT system.

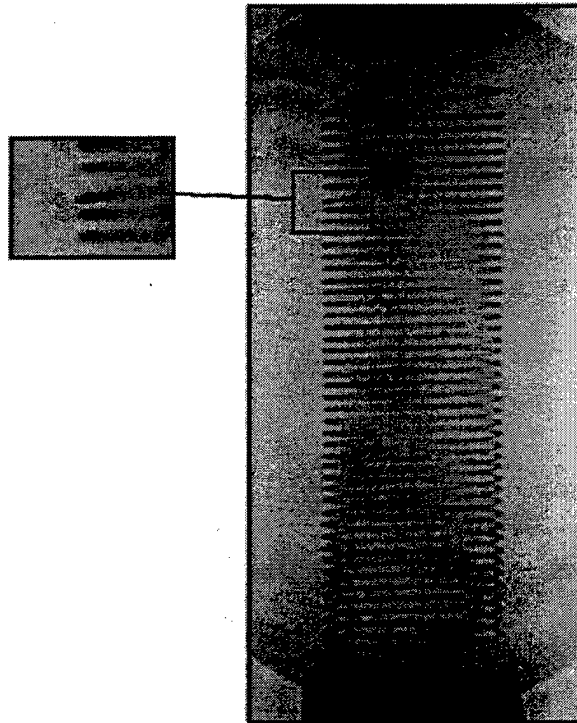


Figure 3.3. Radioscopic image of a wire wound resistor (approximately 1 mm diameter coil) showing improper spacing

While radioscopy is sufficient for evaluation of perhaps 95% or more of the items encountered in a failure analysis laboratory, CT plays a role for approximately 5 % of the workload. A temperature sensor, used in aircraft systems, is an example where the radioscopic imaging becomes inadequate. Figure 3.4 is a photograph of the temperature sensor. The device contains electrical leads to which small (0.025 mm) platinum wires are attached. In nonfunctioning sensors, engineering and manufacturing organizations want to know the cause of the failure. Figure 3.5 is a radioscopic image that clearly shows a broken wire connection.

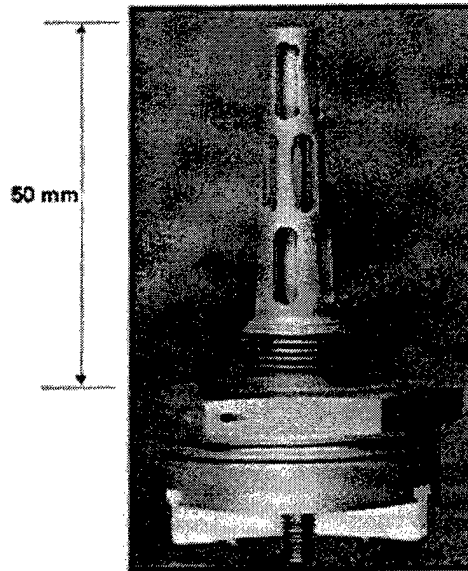


Figure 3.4. Photograph of an aircraft temperature sensor



Figure 3.5. Radioscopic image of a temperature sensor showing a broken wire

Sometimes, however, the location of a failure is such that the radioscopic image cannot detect the problem. Figure 3.6 shows a radioscopic image of a different temperature sensor which had failed. The wire is shown adjacent to a lead. The interpretation of the connection of the wire to the lead cannot be made from this radioscopic view alone. In this view, the wire appears to contact the lead, however, the sensor performance indicates that no signal is available. A series of CT slices is taken of the wire/lead connection location. Figure 3.7 shows the CT image sequence where the wire approaches the lead, but does not actually connect to it. From these data the interpretation of a failed wire to lead bond connection can be made.

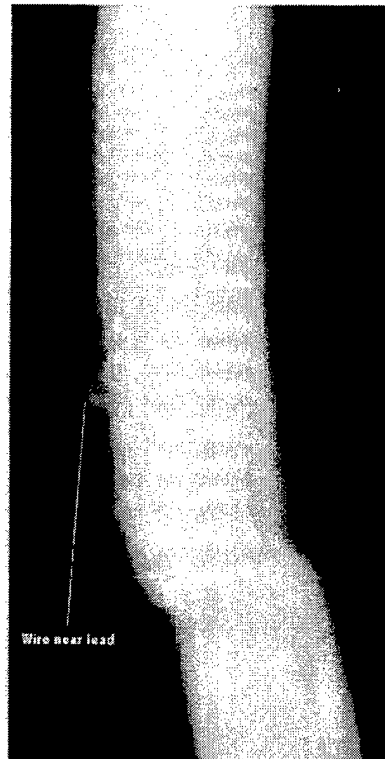


Figure 3.6. Radioscopic image of a temperature sensor showing a wire near a lead

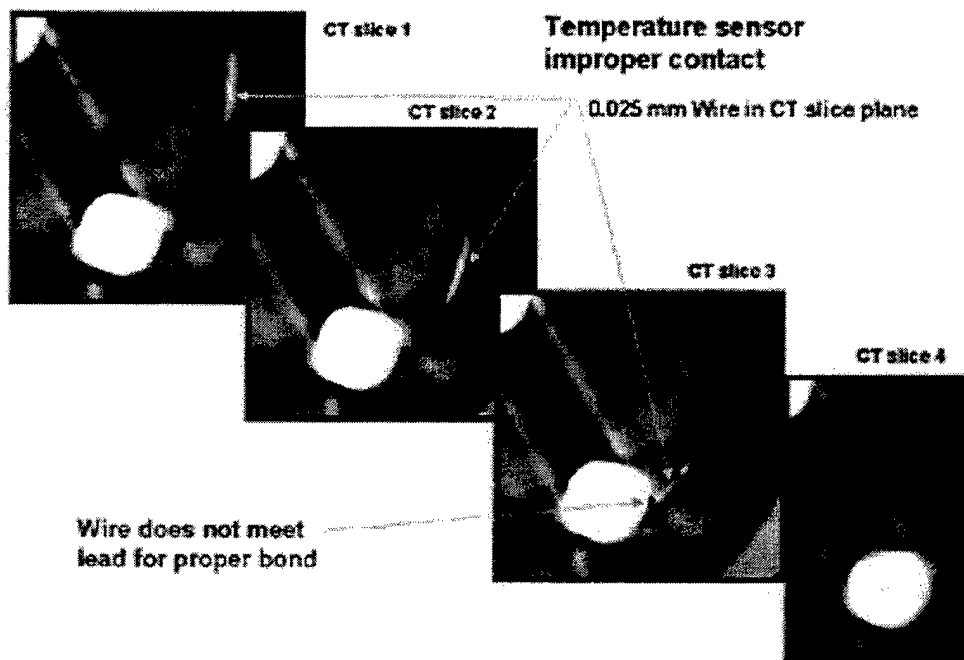


Figure 3.7. CT contiguous image sequence showing the temperature sensor wire failed to connect to the lead

3.2 Connectors And Fiber Optics

Connectors are an area where CT is used very effectively to evaluate the detail fit up of the components when investigating inadequate connector performance. Fiber optic splices are also an example of small components that are essentially impossible to evaluate without destroying the part and often the information desired. Figure 3.8 shows the configuration of the CT system for evaluating fiber optic splices. The fiber optic is spliced by feeding each fiber into the space between four glass rods, held in a metallic tube, from opposite ends. When the fibers touch, a connection is made and the metal tube is crimped to hold the cables. Observing the condition of the connection nondestructively can only be accomplished by CT. The CT slice will show the metal sleeve with the interior glass rod guides. The fiber optic will be in the center of the glass rods. By taking a series of CT slices along the connection, the condition of the fiber optic joint can be assessed. Because the fiber optic is only 0.15 mm in diameter, high resolution CT is required to detect the detail of interest.

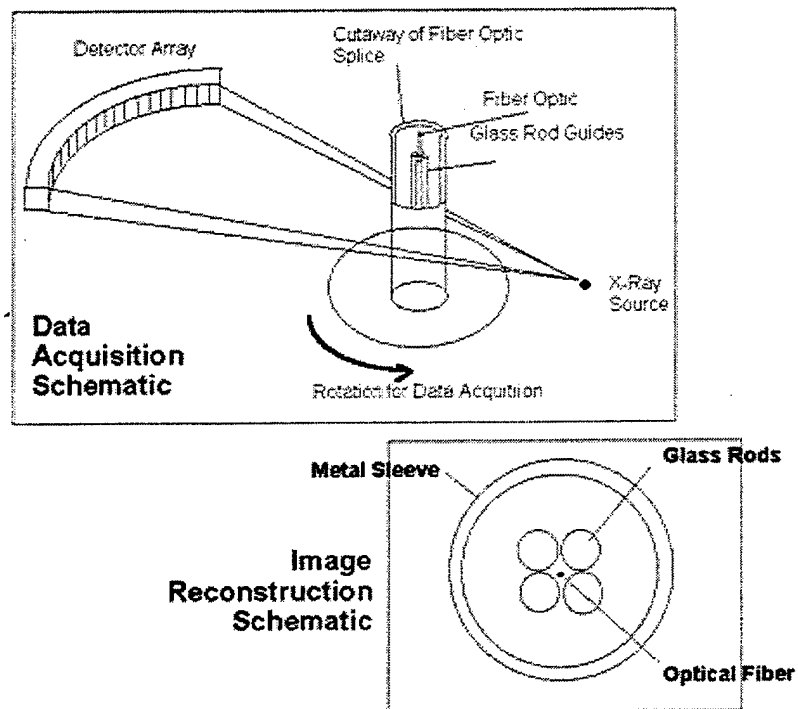


Figure 3.8. Configuration of high resolution CT to evaluate a fiber optic connection

Figure 3.9 shows an example CT evaluation of the fiber optic splice. The upper left image shows the full CT slice of the connector with the metal sleeve and a swage ring. Below is a series of CT slices zoomed in to reconstruct only the glass rods and the fiber optic. The fiber optic is located between the four glass rods in slice 1 and slice 4, but is missing in slices 2 and 3. This gap where the two fibers should come together, explains the poor performance of this connection.

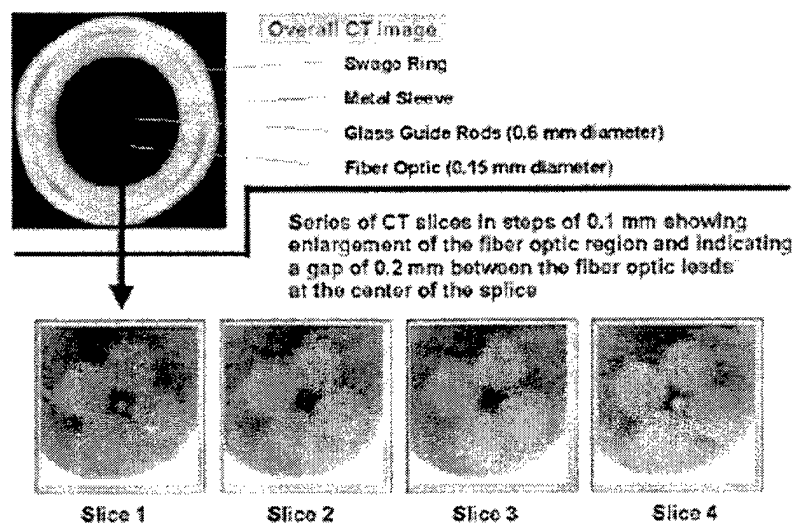


Figure 3.9. CT data from a fiber optic splice

In order to evaluate the internal configuration, the series of contiguous CT slices can be reconfigured. The series of slices form a three-dimensional data set which can be viewed from any orientation. This is called multiplanar reconstruction (MPR). Figure 3.10 shows this type of data. The top image is an axial slice through the splice. The bottom two images are MPR images. These reconstructions view the fiber along its length to show the fiber condition at the splice point, where two fibers should come together and touch. One image shows a misalignment of the two fibers and the other shows that they do not touch (the data of Figure 3.9). Such measurements are not possible by any other means.

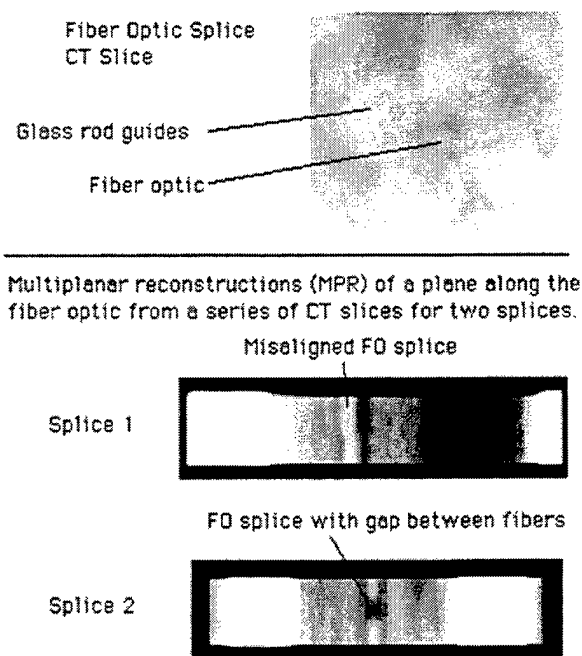


Figure 3.10. CT data from a fiber optic splice showing MPR views of two bad splices

3.3 Composite And Metallic Structure

Samples that are normally evaluated for micrographic analysis can often benefit from nondestructive CT analysis. Figure 3.11 shows the results of a CT evaluation for a resin transfer molded composite T sample. CT data were taken for 127 contiguous slices each 0.25 mm thick with a 19 mm field of view. Using multiplanar reconstruction, the CT slices are combined into a volumetric model of the part and then viewed in orthogonal slices through the volume data set. In the upper left corner of the Figure 3.11 data is the standard CT slice (#17 of the 127). The upper right and lower left are side and front views through the data set. An oblique view is shown in the lower right; its orientation is given by the angled dotted line on the upper left CT image. The Figure 3.11 data show a crack in the radius of the sample and how the crack propagates around the woven composite structure.

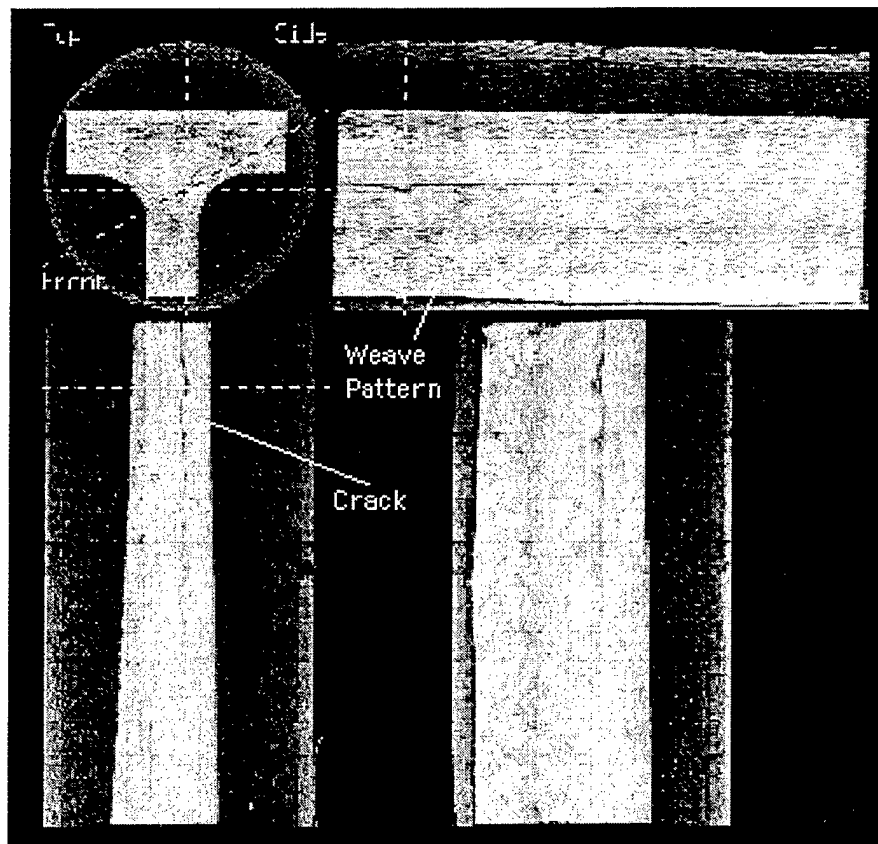
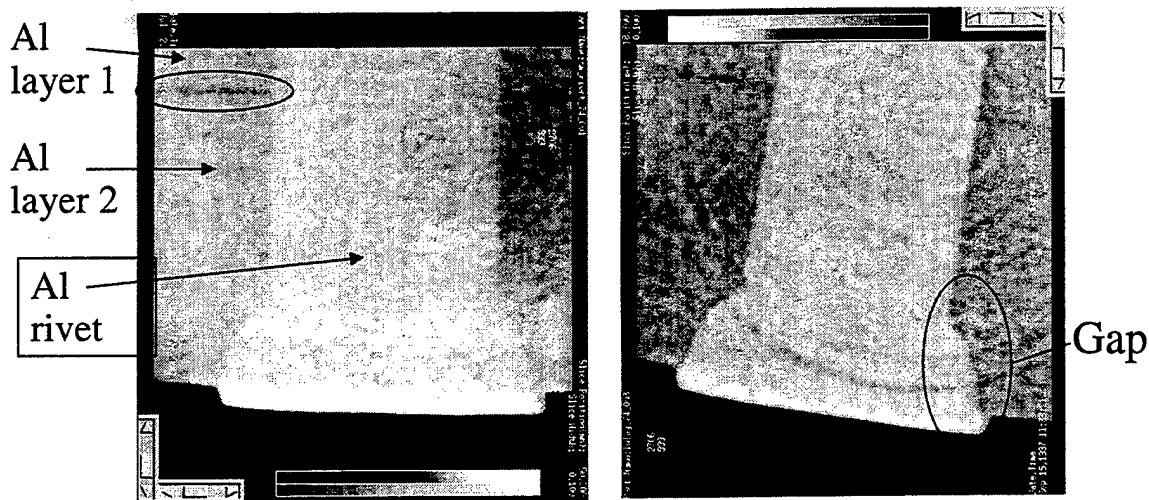


Figure 3.11. CT data from a composite sample

Rivets in aircraft structures have been traditionally evaluated using micrographic studies (13). The rivet is sectioned and evaluated for fit up as a function of processing parameters. CT scanning of the rivet as shown in Figure 3.12 shows that the pre and post sectioning condition of the rivet changes due to stress relief. In Figure 3.12 the presectioning image shows no significant gap between the rivet and the aluminum layer. A gap is detected between the two aluminum layers. In the post sectioned image of a rivet, taken just below

the cut surface, a gap is shown in the CT image between the rivet and the aluminum layer around the rivet head. Photomicrographs of the cut specimen noted 0.050 mm (0.002 inch) wide gaps. The CT post sectioned scan indicated 0.050 to 0.075 mm (0.002 to 0.003 inch) gaps at this location indicating that the gaps are a result of sectioning. These results clearly indicate that using the micrography data on a sectioned rivet to establish the condition present prior to sectioning is not correct. Rather, nondestructive evaluation can produce a more accurate description of the true part condition. Although the micrographic images have greater resolution than the CT data, the data are not a valid representation of the as-riveted condition. Sectioning relieves stresses resulting in a change in the true geometry of a structure.



a) Pre sectioning CT image showing no gaps b) Post sectioning image shows gaps

Figure 3.12. CT scan of rivet a) pre sectioning and b) post sectioning

CT slices have also been generated perpendicular to the longitudinal axis (circumferentially) to see if the detectable gaps were consistent around the entire rivet. The data generated show that the gaps are not consistent around the entire circumference. This result further indicates that traditional sectioning may not be representative of the entire rivet condition.

Another example of the use of high resolution CT on metallic structure is one that the benefits of CT prior to the test were thought to be dubious at best. This example is a small pressure reservoir that was leaking, but the leak could not be detected by other than a leak test. CT was used and a crack detected as shown in Figure 3.13. A series of CT slices was taken and displayed in MPR to show the orientation of the crack in the reservoir wall.

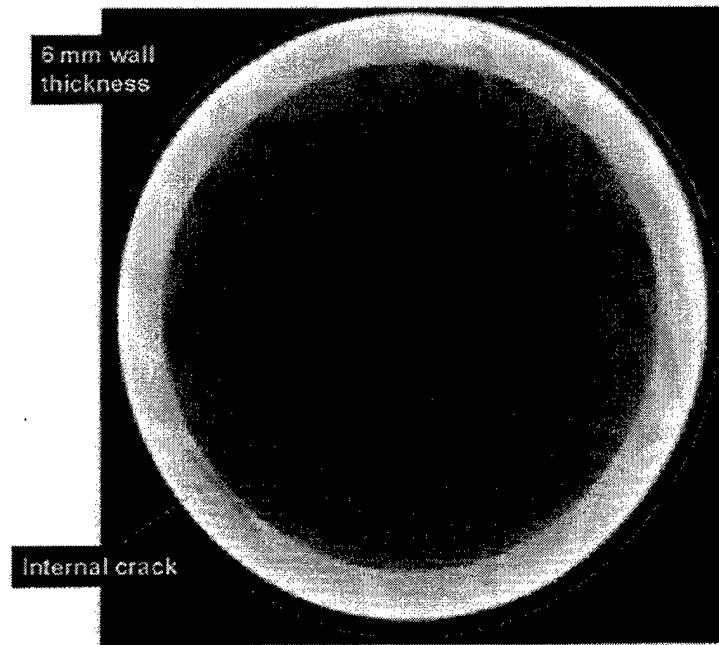


Figure 3.13. CT slice through the reservoir showing the crack

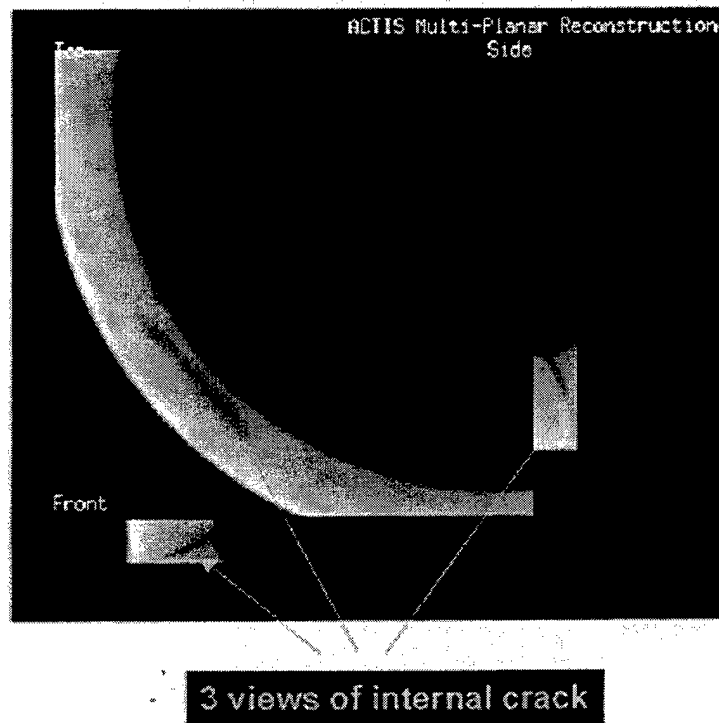


Figure 3.14. MPR of the crack in the reservoir

4.0 COST BENEFIT ANALYSIS

The acquisition of a microfocus radiography/CT system involves a significant investment above the cost of a film radiography system. The equipment may cost between \$400K to \$700K. The justification of such equipment must be sufficient to compensate for the investment. Estimating the cost benefit of radioscopic/CT system, relative to not having the capability requires some assumptions which are often difficult to quantify. For example, what is the value of a wrong evaluation? And, what is the risk of a bad evaluation if inadequate equipment is used? While there is no simple answer to these questions, a computation can be made in several ways on the cost benefit of a system.

The first approach in estimating the value of the system is to ask if there is a direct reduction in manpower effort with the capability. In the case of a failure analysis laboratory that deals primarily with electronic and electro-mechanical devices, an estimate can be made based on experience. In the case of the Boeing Information Space & Defense Systems Failure Analysis Laboratory, the use of the radioscopic imaging capability has become the second step, following log-in and photography, of the failure analysis procedures for nearly all projects. By visualizing the internal configuration prior to any disassembly procedures, errors are reduced or eliminated and savings result. The manipulation of the object under radioscopic examination provides visualization of the interior from all orientations. In some cases, these images are sufficient to complete the report. In most cases these data guide the subsequent process. For a failure analyst, the effect of the rapid imaging at very high sensitivity to fine detail provides the equivalent of a day's work (prior to the availability of MRCT capability) in less than an hour. While on particular parts the benefits of the MRCT are substantial, the system appears on average, over the total workload, to reduce the evaluation effort by about 10%. In a simple payback scenario of 5 years for a \$600K system, then the savings would need to be at least \$120K/year. This would take place in a laboratory whose annual work effort was around \$1.2M/year. Thus, a laboratory staffed with 6 to 10 people would be a candidate for investing in an MRCT system.

Another estimate of the payback of MRCT is to ask what the evaluations would cost if the system was not present in the laboratory. Take, for example, a laboratory that might perform 500 failure analysis investigations/year. Each investigation may require a number of detailed steps, and/or a number of parts such that on average the investigations consume about three quarters of a week of labor. The MRCT capability is applicable to approximately 80% of the investigations. In general, the procedure is to perform a quick X-ray evaluation (1 hour) on most parts, ascertaining the internal condition, prior to opening. On approximately half of the jobs the quick look may become a more detailed (4 hours) study. The total work load is then on the order of $(500 \times 0.8 \times 0.5 \times (1 + 4)) = 1000$ hours of effort. If this work were to be performed by a third party examination facility the costs would be expected to be in the range \$150/hr. This translates into \$150K/year, or again an approximately 4 year payback for a \$600K system.

A third cost benefit analysis that is appropriate for failure analysis laboratories is the effect on schedule. Often in the aerospace industry, failure analysis is critical to decision making during a project or for a system that is in service. Schedule for important projects can be of

much greater value than the parts themselves. For example, an aircraft-on-ground (AOG) situation can cost \$150K/day. A production stop situation is estimated at \$100K/day in the aerospace industry. If a MRCT system were to save a half of a day of schedule in an AOG or production work stop situation a few times a year the investment in the system would be justified by reducing the total payback time to a year or two.

The above techniques provide a justification of a MRCT system using simple payback calculations. Figure 4.1 summarizes the techniques. The right side of Figure 4.1 lists the parameters that are used for the calculation of payback issues. More sophisticated models could be used, however, the accuracy of the values available for the models are such that the simple calculations are sufficient. In the case of the first two techniques, a 5-year payback is used, indicating that large (greater than 320 jobs/year and \$1.2M/year work effort) failure analysis laboratories could justify systems. A 5-year simple payback, however, is probably insufficient justification when capital resources are in competition between projects in large corporations. The effect of critical jobs, however, shows that the payback can be significantly enhanced. To show a 2-year simple payback, a laboratory would need to support approximately 1 out of 100 jobs related to critical problems (such as AOG and production stop work) where the effect of the laboratory is a half a day of schedule savings. Such a justification is likely to be very conservative for laboratories in major corporations.

| Cost Benefits Assessment Techniques | |
|--|--|
| Technique 1 Yearly workload effort Y MRCT system cost = P = \$600K Work Saving = S = 10% | Laboratory size to justify system over 5 years is : $Y = (P/5)/S$ $Y = (\$600K/5\text{yr}/0.1)$ $Y = \$1200K/\text{yr}$ |
| Technique 2 MRCT system cost = P = \$600K Number of jobs that could use MRCT = N Cost of outside work/hr = C = \$150/hr Probability of long jobs = p = 0.5 Length of MRCT effort for long jobs = t1 = 4 hrs Length of MRCT effort for short jobs = t2 = 1 hr | Laboratory effort to justify a system $N = \{P/5\} / \{[t1 \times p + t2 \times (1-p)] \times C\}$ $N = \{\$600K/5\} / \{[4 \times 0.5 + 1 \times 0.5] \times \$150/\text{hr}\}$ $N = 120000/375$ $N = 320$ |
| Technique 3 MRCT system cost = P = \$600K Number of jobs that could use MRCT = N = 320 Probability of AOG job = p1 (let p2 = p1) Probability of production stop work job = p2 Value of AOG schedule = V1 (0.5 x \$150K = \$75K) Value of production stop work = V2 (0.5 x \$100K = \$50K) | Probability of AOG and stop work production jobs to justify a system over 2 years $p1 = \{P/2\} / (V1 \times N + V2 \times N)$ $p1 = (\$600K/2) / (\$75 \times 320 + \$50K \times 320)$ $p1 = 300/40,000$ $p1 = 0.0075$ |

Figure 4.1. Simple cost benefit payback techniques for MRCT system

The presence of a MRCT system also has the effect of increasing business for a failure analysis laboratory. The speed and accuracy of the system for measurements on components increases the inspection of electrical/electronic items considerably. Because of the benefits of using MRCT on projects of high economic value, MRCT equipment often can pay for itself several times over in the matter of less than 2 years. The principal paybacks come from the equivalent work force activity of 1 person per year, the beneficial resolution of high value litigation studies and the support of component evaluation for critical missions by saving

schedule. Overall, these paybacks are realized because the MRCT system provides higher quality information than was available prior to its acquisition. A failure analysis laboratory is driven by customer satisfaction. Having high quality information available rapidly is a key to success. The investment in such equipment can be repaid very rapidly.

5.0 RECOMMENDATIONS

Microfocus radioscopy and CT offer detailed information on internal object assembly and material condition which, when utilized in a failure analysis investigation, reduces the overall effort while improving the failure analysis assessment accuracy. The microfocus X-ray source provides projection magnification images that exceed the sensitivity to fine detail that can be obtained with conventional film radiography. A versatile MRCT system can pay for itself within 2 years through higher productivity of the laboratory, increased laboratory value to the company and resolution of critical component problems whose worth exceeds the cost of the microfocus radioscopy/CT system. The Air Forces should consider the availability of such equipment as essential tools for contractors who work on Air Force programs.

Improvements in the system, imaging technology and the data handling could increase the value of a MRCT systems even more. Higher energy and greater output microfocus sources would improve overall performance with greater X-ray flux and applicability to larger (or more dense) objects. A robot manipulator for remote functioning of switches would be a welcome addition to a system. Digital x-ray detector schemes such as amorphous silicon should be developed to replace image intensifiers. This technology will increase dynamic range of the detector, increasing sensitivity and reduce blooming problems in imaging. The digital detector scheme provides an inherently flat image field which overcomes the problem of the curved image intensifier input screen and subsequent variable sensitivity across the intensifier field of view. Rapid volume CT reconstruction developments should be pursued to assemble a system that performs CT over an entire part at speeds that could reduce inspection times by several orders of magnitude.

The information generated in this program has been distributed to industry and government through presentations/publications in various forums. Three presentations with published technical paper proceedings have been made on the topic to JANNAF, SPIE and ISTFA. A presentation was also made at the ASNT Fall Conference in 1998 and a paper is in review for the *Journal of Testing and Evaluation*.

6.0 REFERENCES

1. L. Bryant, ed. *Nondestructive Testing Handbook*, Volume 3 "Radiography and Radiation Testing," Second Edition, American Society for Nondestructive Testing, 1985 pp. 801-807.
2. R. Bossi, C. Oien, and P. Mengers, "Real Time Radiography," *Nondestructive Testing Handbook*, Volume 3 "Radiography and Radiation Testing," L. Bryant, ed. Second Edition, American Society for Nondestructive Testing, 1985.
3. M. J. Dennis, "Industrial Computed Tomography," *Metals Handbook*, Volume 17, "Nondestructive Evaluation and Quality Control," ASM International, 1989.
4. D. Copley, J Eberhard and G. Mohr, "Computed Tomography Part 1: Introduction and Industrial Applications," *Journal of Materials*, January 1994.
5. ASTM, "Standard Guide for Computed Tomography (CT) Imaging," E 1570 - 93 American Society for Testing and Materials, 1993.
6. R. Bossi, D. Cross and R. Mickelsen, "X-Ray Microfocus Radioscopy and Computed Tomography for Failure Analysis", ASM ISTFA, Anaheim, CA, November 1996.
7. ASTM, "Standard Guide for Radioscopy" E 1000 - 92 American Society for Testing and Materials, 1992.
8. R. H. Bossi and L Deobald, "Radioscopic Imaging of E-Beam Welds," American Society for Nondestructive Testing, Fall Conference, Dallas, TX, 1995.
9. R. Bossi, J. Cline and G. Georgeson, "High Resolution Computed Tomography," WL-TR-91-4102, July 1992.
10. R. Bossi, A. Crews and G. Georgeson, "X-Ray Computed Tomography for Failure Analysis," WL-TR-92-4017, August 1992.
11. R. Bossi and W. Shepherd, "X-Ray Computed Tomography for Failure Analysis Investigations," WL-TR-93-4047, May 1993.
12. R.H. Bossi, K.D. Friddell and A.R Lowrey, "Computed Tomography," in *Non-Destructive Testing of Fibre-Reinforced Plastics Components*, Vol. 2, John Summerscales, Ed., Elsevier Applied Sciences, London, 1990.
13. K.E. Lulay, G.E. Georgeson, and P. Kostenick, "X-ray Computed Tomography for Verification of Rivet Installation Assessment Techniques," SAE Aerofast, Sept 15-17, 1998.